

Double Ion Production in Argon and Xenon Ion Thrusters

Paul J. Wilbur* and Harold R. Kaufman†
Colorado State University, Fort Collins, Colo.

A model describing the doubly charged ion densities in argon and xenon ion thrusters is presented. Doubly charged ions are shown to be produced in significant numbers from both the neutral and singly ionized states. Doubly-to-singly charged ion density ratios calculated using this model are compared to experimental values of this ratio measured in the 15-cm multipole thruster, using both propellants. Agreement between theory and experiment is shown to be good.

Nomenclature

A	= surface area, m^2
e	= electron charge, C
F	= uniformity factor
m	= mass, kg
n	= specie density, m^{-3}
P	= primary electron rate factor, m^3/s
Q	= Maxwellian electron rate factor, m^3/s
R	= rate of specie formation or loss, s^{-1}
T	= temperature, eV
v	= velocity, m/s
V	= volume, m^3
ξ	= energy, eV
σ	= cross section, m^2

Superscripts

+	= singly charged ion
++	= doubly charged ion

Subscripts

+	= singly charged ion
++	= doubly charged ion
e	= electron
i	= ion
l	= loss
Mx	= Maxwellian electron
0	= neutral atom
p	= primary electron region
pr	= primary electron

Introduction

DOUBLY charged ions have been found to be undesirable in the discharge chambers of mercury electron bombardment ion thrusters, primarily because they increase the rate of sputtering damage to discharge-chamber components. As gaseous propellant thrusters are developed, one would expect that sputtering damage from the doubly charged ions of these propellants might be also encountered. A theoretical model describing the densities of doubly charged ions as a function of discharge chamber conditions should facilitate the estimation of erosion rates of critical, life-limiting thruster components by a designer. The purpose of this paper is to develop such a model and verify its accuracy experimentally.

Presented as Paper 78-667 at the AIAA/DGLR 13th International Electric Propulsion Conference, San Diego, Calif., April 25-27, 1978; submitted June 30, 1978; revision received Jan. 22, 1979. Copyright © 1978 by P. J. Wilbur. Published by the American Institute of Aeronautics and Astronautics with permission.

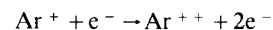
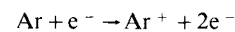
Index category: Electric and Advanced Space Propulsion.

*Associate Professor, Department of Mechanical Engineering.

†Professor, Departments of Physics and Mechanical Engineering.

Theoretical Model

The ion discharge chamber model developed by Peters¹ for application to mercury thrusters provides the basis for this work. In this model, the production rate of doubly charged ions is equated to their loss rate and the production rate is presumed to include contributions due to direct ionization of neutral atoms to the doubly ionized state as well as significant multiple step processes involving intermediate states. For the case of mercury propellant as analyzed by Peters, the important intermediate steps included several resonance and metastable states. For argon and xenon, however, a relatively large energy interval exists between the atomic and ionic ground states and the lowest metastable and resonance states. This suggests that metastable and resonance states will not be important in the analysis, and their effect is therefore neglected in this development. For argon, then, the only reactions which are considered in determining the doubly charged ion production rate are



The reactions for xenon are the same as those shown above, and the equations developed in succeeding pages will therefore be applicable to both of these propellants.

The electrons which induce the ionizing reactions are assumed to consist of a Maxwellian group and a monoenergetic or primary group, in accordance with the findings of Isaacson² that such a two-electron-group model appears to describe an argon or xenon plasma.

The differential rate of production of singly charged ions from neutral atoms affected by electrons with velocities between v and $v+dv$ having a density dn_e within a volume dV is given by

$$d^2R_0^+ = n_0 v \sigma_0^+ dn_e dV \quad (1)$$

Integration of Eq. (1) yields the rate of production of singly charged ions from neutral atoms,

$$R_0^+ = n_0 V_p [n_{pr} P_0^+(\xi_{pr}) + n_{Mx} Q_0^+(T_{Mx})] \quad (2)$$

where the densities, energies, and temperatures used in this equation are averaged values obtained through the application of appropriate weighting factors as defined by

Peters.¹ The quantities $P_{\theta}^{+}(\xi_{pr})$ and $Q_{\theta}^{+}(T_{Mx})$ represent the electron velocity-cross section product for the primary and Maxwellian electron groups respectively, integrated over the distribution functions for these groups. It has been assumed in this development that the bulk of the reactions occur within the primary electron region, so its volume V_p appears in Eq. (2).

Equations for the production rates via the neutral-to-doubly ionized and singly-to-doubly ionized reactions are identical to Eq. (2) except for the fact that they include the rate factors pertaining to these reactions in place of $P_{\theta}^{+}(\xi_{pr})$ and $Q_{\theta}^{+}(T_{Mx})$. The rate factors describing each of the production reactions have been computed as a function of primary electron energy and Maxwellian electron temperature for both argon and xenon and they are presented in Table 1. The cross section for the neutral-to-singly charged and neutral-to-doubly charged reactions required for these computations were obtained from experimental results as reported by Kieffer and Dunn.³ The cross sections describing the singly-to-doubly charged reactions were obtained analytically, using the classical cross section model of Gryzinski.⁴

The loss rate for doubly and singly charged ions from the plasma is due almost entirely to ion migration to the discharge plasma boundary. Such a boundary could be either a section of the discharge chamber wall on which the ion would recombine or it could be a grid aperture through which the ion would be extracted into the ion beam. In either case, neutral atoms are returned to the discharge chamber from the chamber walls or the propellant supply system to maintain the neutral density constant. These ion loss rates are given by equations of the form

$$R_i^{+} = n_{+} v_{+} A_p \quad (3)$$

The ion velocity appearing in this equation is determined from the Bohm criterion for a stable sheath.⁵ An equation similar to Eq. (3) is obtained for the doubly charged ions, using the same logic as that which has been discussed for singly charged ions.

At equilibrium the rate of production of each ionic specie must equal its loss rate, so Eqs. (2) and (3) may be equated and combined with the Bohm equation, describing the ion velocity, to obtain the ratio of the average atom density to the

singly charged ion density:

$$\frac{n_0}{n_{+}} = \frac{[(e/m_i) T_{Mx} (1 + n_{pr}/n_{Mx})]^{1/2}}{[V_p/A_p] [F_{+}] [n_{pr} P_{\theta}^{+}(\xi_{pr}) + n_{Mx} Q_{\theta}^{+}(T_{Mx})]} \quad (4)$$

The plasma uniformity factor F_{+} is the ratio of the volume-averaged singly charged ion flux to the singly charged ion flux averaged over the surface area of the plasma boundary. It can be calculated from discharge chamber plasma properties measured throughout the discharge chamber in the manner described by Peters.¹

When the total production rate of doubly charged ions due to ionization of both neutral and singly charged ions is equated to the loss rate of doubly charged ions, the following expression is obtained:

$$\frac{n_{++}}{n_{+}} = \frac{X}{[2T_{Mx} (e/m_i) (1 + n_{pr}/n_{Mx})]^{1/2}} \quad (5)$$

where

$$X = (V_p/A_p) F_{++} \{ n_{pr} [P_{++}^{+}(\xi_{pr}) + (n_0/n_{+}) P_{\theta}^{++}(\xi_{pr})] + n_{Mx} [Q_{++}^{+}(T_{Mx}) + (n_0/n_{+}) Q_{\theta}^{++}(T_{Mx})] \}$$

It is observed to be similar to Eq. (4) except for the appearance of additional terms which reflect the fact that doubly charged ions can be produced via two routes (directly from atoms or from singly charged ions). Equation (5) also includes the plasma uniformity factor for doubly charged ions F_{++} . This factor is the ratio of the volume-averaged doubly charged ion flux to the doubly charged ion flux averaged over the surface area of the plasma boundary.

The application of this model requires a knowledge of the volume-averaged plasma properties and the geometry of the primary electron region in the discharge chamber being examined. The plasma properties are used to enter Table 1 and determine the appropriate rate factors. Substitution of these factors and the plasma and geometric properties into Eq. (4) gives the neutral-to-singly charged ion density ratio. Substitution of the same plasma and geometric factors together with the rate factors called for in Eq. (5) and the ratio determined from Eq. (4) into Eq. (5) enables one to calculate the average double-to-singly charged ion density ratio for the thruster.

Model Verification

A 15-cm-diameter multipole thruster was built and tested by Isaacson² using xenon and argon propellants. The length of this thruster and the propellant flow rate to it were varied. Plasma properties were measured throughout the discharge chamber, using a movable Langmuir probe for each test configuration. At essentially the same time as these plasma measurements were being made, the singly and doubly charged ion current density profiles were measured in the ion beam, using a mass spectrometer. From the resultant data, the volume-averaged plasma properties, plasma uniformity factors, and doubly-to-singly charged ion density ratios were determined. The thruster operating conditions, volume-averaged plasma properties, measured doubly-to-singly charged ion density ratios, and results calculated from Eqs. (4) and (5) are given in Table 2. Rows 14 and 15 of this table show the values of average doubly-to-singly charged ion density ratio 1) computed from measured plasma properties and 2) determined from doubly and singly charged ion current density measurements in the beam. These data are also plotted in Fig. 1. Each data point in the figure corresponds to a

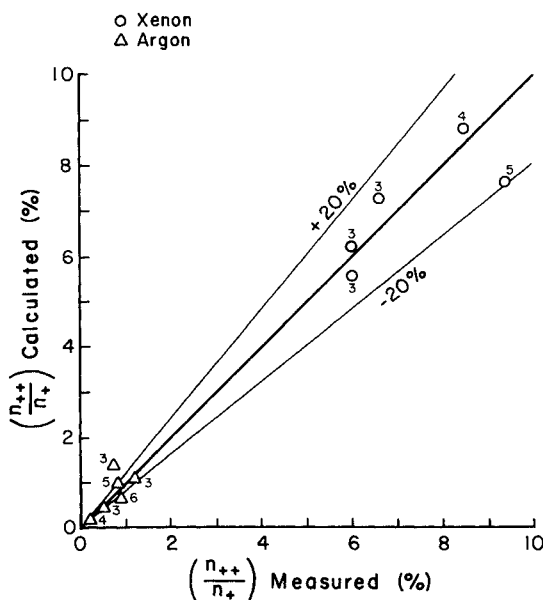


Fig. 1 Comparison of theory and experiment for double-to-single ion density ratio.

Table 1 Rate factors

T_{Mx}, eV	$Q_0^+, \text{m}^3/\text{s}$	$Q_0^{++}, \text{m}^3/\text{s}$	$Q_+^{++}, \text{m}^3/\text{s}$	ξ_{pr}, eV	$P_0^+, \text{m}^3/\text{s}$	$P_0^{++}, \text{m}^3/\text{s}$	$P_+^{++}, \text{m}^3/\text{s}$
Argon							
3	0.019×10^{-14}	...	0.0001×10^{-14}	5
4	0.086	...	0.002	10
5	0.22	...	0.008	15	0.002×10^{-13}
6	0.41	0.004×10^{-15}	0.025	20	0.17
7	0.66	0.012	0.053	25	0.39
8	0.95	0.029	0.097	30	0.60	...	0.245×10^{-14}
9	1.26	0.057	0.15	35	0.77	...	1.04
10	1.58	0.099	0.23	40	0.89	...	1.90
12	2.25	0.23	0.40	45	0.99	0.05×10^{-14}	2.76
15	3.24	0.55	0.73	50	1.06	...	3.55
18	4.15	0.99	1.10	60	1.15	0.44	4.89
21	4.98	1.52	1.49	70	1.26	0.75	5.94
24	5.72	2.10	1.88	80	1.32	1.07	6.73
27	6.38	2.71	2.25	90	1.35	1.32	7.33
30	6.98	3.33	2.61	100	1.33	1.45	7.83
Xenon							
3	0.009×10^{-13}	...	0.002×10^{-14}	5
4	0.032	0.0003×10^{-14}	0.014	10
5	0.071	0.0018	0.051	15	0.13×10^{-13}
6	0.12	0.0063	0.12	20	0.63
7	0.18	0.016	0.23	25	1.00	...	0.071×10^{-13}
8	0.24	0.032	0.37	30	1.29	...	0.25
9	0.31	0.055	0.53	35	1.51	0.065×10^{-14}	0.42
10	0.37	0.085	0.73	40	1.64	0.50	0.57
12	0.50	0.166	1.16	45	1.74	1.27	0.69
15	0.67	0.327	1.89	50	1.79	1.86	0.80
18	0.82	0.517	2.63	60	1.82	2.64	0.97
21	0.95	0.721	3.35	70	1.97	3.20	1.09
24	1.06	0.925	4.02	80	2.10	3.63	1.18
27	1.16	1.13	4.65	90	2.18	3.99	1.24
30	1.25	1.32	5.22	100	2.19	4.36	1.29

Table 2 Test conditions and results

Propellant	Ar	Ar	Ar	Ar	Ar	Xe	Xe	Xe	Xe	Xe
Length, cm	8.1	8.1	10.8	13.5	16.2	8.1	8.1	8.1	10.8	13.5
Flow rate, mA	643.	951.	640.	638.	676.	211.	425.	626.	420.	420.
Discharge current, A	3.0	4.5	3.1	3.0	3.1	1.5	2.5	3.5	3.6	4.0
Discharge voltage, V	50.	50.	50.	50.	50.	45.	45.	45.	45.	45.
T_{Mx}, eV	17.7	12.4	14.9	12.4	7.1	15.8	10.8	6.8	10.4	10.9
ξ_{pr}, eV	52.6	49.1	52.8	56.6	46.2	51.5	48.5	48.4	47.5	44.7
$n_{Mx}, \text{m}^3 \times 10^{-16}$	2.02	3.76	2.74	3.17	3.05	2.60	7.30	15.6	8.03	9.28
$n_{pr}, \text{m}^{-3} \times 10^{-15}$	2.81	2.55	0.41	3.39	2.82	5.98	5.59	7.52	9.43	6.17
$V_p/A_p, \text{m}$	0.020	0.020	0.022	0.24	0.025	0.020	0.020	0.020	0.022	0.024
F_+^{++}	4.76	4.27	8.01	9.06	11.2	4.84	6.15	5.18	4.26	10.1
F_+	7.17	4.05	5.48	49.3	16.9	4.72	5.97	5.06	2.38	40.0
Calculated n_0/n_+	44.5	60.9	54.4	4.34	20.3	14.0	6.08	5.90	11.4	0.606
Calculated n_{++}/n_+	0.014	0.011	0.002	0.010	0.007	0.073	0.062	0.056	0.088	0.076
Measured n_{++}/n_+	0.007	0.012	0.002	0.008	0.009	0.066	0.060	0.060	0.085	0.094
Fraction of doubly charged ions produced from:										
Neutral atoms	0.77 (0.26)	0.76 (0.27)	0.80 (0.06)	0.22 (0.58)	0.32 (0.87)	0.75 (0.55)	0.50 (0.54)	0.49 (0.84)	0.65 (0.64)	0.05 (0.07)
Singly charged ions	0.23 (0.34)	0.24 (0.34)	0.20 (0.08)	0.78 (0.51)	0.68 (0.81)	0.25 (0.47)	0.50 (0.40)	0.51 (0.64)	0.35 (0.53)	0.95 (0.34)

measured and calculated density ratio for a different thruster length or flow rate. The 45 deg line drawn through the data corresponds to perfect correlation between the results of the model and the measured doubly-to-singly charged ion density ratios. The data of Fig. 1 are seen to lie close to the 45 deg line with all but one point enclosed within the $\pm 20\%$ band. The number next to each data point is the number of multipole thruster side sections on the thruster configuration used in the corresponding test. The number four, for example, indicates that four side sections were used, and since each section is 2.7 cm long, this configuration would have had a total length of 10.8 cm.

Doubly-to-singly charged ion density ratios were observed to be much lower with argon than they were with xenon. This can be seen in the data of Fig. 1. The model shows that the reason for this is the smaller argon cross sections and the lower argon atomic mass, both of which appear in the numerator of Eq. (5).

Consideration of the relative magnitude of each of the terms of Eq. (5) shows the relative contribution of each of the processes and ionizing species considered in the analysis. The results of such an examination are given in rows 16 and 17 of Table 2. Each column of these rows contains two numbers. The first number shows the fraction of the doubly charged ion production reactions involving each of the species indicated (atoms or singly charged ions). This number is followed by a second one (in parentheses) indicating the fraction of these reactions effected by primary electrons. For example, in the 8.1-cm-long argon chamber at 643 mA flow rate, 77% of the doubly charged ions are produced through reactions with neutral atoms and 26% of these reactions are induced by primary electrons; the remainder of the doubly charged ion reactions (23%) involve singly charged ions and 34% of the reactions are caused by primary electrons. Table 2 shows that doubly charged ions are produced in significant numbers for argon and xenon by both primary and Maxwellian electrons. Further, doubly charged ions are produced by both one-step (atom-to-doubly ionized) and two-step (neutral-to-singly ionized-to-doubly ionized) reactions.

In passing, it is interesting to note that the plasma uniformity factors F_{++} and F_{+} are generally higher and

more random than they have been in previous studies conducted on mercury thrusters.^{1,6} The reason for this may be related to the fact that plasma property gradients are much steeper near the boundary of the primary electron region in the multipole thruster used for these tests than they were for the divergent field thruster used in the previous tests. Such a condition could be expected to cause greater variations in plasma properties because of Langmuir probe positioning uncertainty.

Conclusion

The average density of doubly charged argon and xenon ions in an ion thruster discharge chamber can be calculated using a simple model which considers only neutral, singly ionized, and doubly ionized ground state species. Calculated doubly-to-singly charged ion density ratios agree with measured values to within about $\pm 20\%$. Scatter between measured and calculated values appears to be random rather than systematic.

Acknowledgments

This work was performed under NASA Grant NSG 3011.

References

- ¹Peters, R. R., "Double Ion Production in Mercury Thrusters," NASA CR-135019, April 1976.
- ²Isaacson, G. C., "Multipole Gas Thruster Design," NASA CR-135101, June 1977.
- ³Kieffer, L. J. and Dunn, G. H., "Electron Impact Ionization Cross-section Data for Atoms, Atomic Ions, and Diatomic Molecules: I. Experimental Data," *Reviews of Modern Physics*, Vol. 38, Jan. 1966, pp. 1-35.
- ⁴Gryzinski, M., "Classical Theory of Atomic Collisions, I. Theory of Inelastic Collisions," *Physical Review*, Vol. 138, April 19, 1965, p. A341.
- ⁵Bohm, D., "Minimum Ionic Kinetic Energy for a Stable Sheath," *The Characteristics of Electrical Discharges in Magnetic Fields*, edited by A. Guthrie and R. K. Wakerling, McGraw-Hill, New York, 1949, pp. 77-86.
- ⁶Wilbur, P. J., "Mercury Ion Thruster Research—1977," NASA CR-135317, Dec. 1977, pp. 96-104.